

## Marked Alkyl- vs Alkenyl-Substituent Effects on Squaraine Dye Solid-State Structure, Carrier Mobility, and Bulk-Heterojunction Solar Cell Efficiency

Diego Bagnis,<sup>‡,¶</sup> Luca Beverina,<sup>†</sup> Hui Huang,<sup>‡</sup> Fabio Silvestri,<sup>†</sup> Yan Yao,<sup>§</sup> Henry Yan,<sup>§</sup>  
Giorgio A. Pagani,<sup>\*,†</sup> Tobin J. Marks,<sup>\*,‡</sup> and Antonio Facchetti<sup>\*,‡,§</sup>

Department of Materials Science, Università di Milano-Bicocca, via Cozzi 53, 20125, Milano, Italy, Department of Chemistry and the Argonne-Northwestern Solar Energy Research Center, Northwestern University, Evanston, Illinois 60208, Polyera Corporation, 8045 Lamon Avenue Skokie, Illinois 60077, Department of Civil and Environment Engineering, Università di Perugia, NIPLAB-INSTM, Via Pentima Bassa 21, 05100 Terni, Italy

Received January 27, 2010; E-mail: a-facchetti@northwestern.edu; giorgio.pagani@mater.unimib.it; t-marks@northwestern.edu

Bulk-heterojunction organic photovoltaic (BHJ-OPV) cells exhibiting high power conversion efficiencies (PCEs) may provide inexpensive, renewable sources of solar electricity via low-temperature fabrication on flexible substrates, impossible for silicon.<sup>1</sup> In such devices, the photoactive layer consists of a phase-separated donor-acceptor semiconductor blend that provides interfaces for exciton splitting and networks for hole and electron transport to the electrodes.<sup>2,3</sup> An attractive approach to increasing PCEs includes, besides developing unconventional device structures and contact/interfacial materials,<sup>4</sup> exploring new photoactive semiconductors, particularly BHJ donors.<sup>5</sup>

In recent years, new molecular polymeric BHJ-OPV donor material classes have been discovered and implemented with the fullerene acceptors PC<sub>61</sub>BM and PC<sub>71</sub>BM. Their characterization provides fundamental information on how  $\pi$ -system modifications affect PCE by altering light absorption, active layer microstructure, exciton dynamics, and carrier mobility. These results raise the interesting question of how subtle  $\pi$ -core substituent variations, which marginally affect solution phase molecular properties, might promote significantly different OPV responses.

We report here the synthesis and remarkable property differences of two new squaraine dyes, substituted at the pyrrolic nitrogen with *n*-hexyl (squaraine **1**) or *n*-hexenyl (squaraine **2**) chains (Figure 1). These derivatives are synthesized via modifying previously reported procedures,<sup>6</sup> condensing the appropriate arylhydrazone-alkylpyrroles with squaric acid in ~42% (**1**) and ~52% (**2**) yield, respectively. The new compounds were characterized by conventional spectroscopic/analytical/X-ray diffraction methodologies (see Supporting Information). Although internal molecular structure variations are minimal, the data reveal that the *N*-alkenyl substituent affords a more compact solid-state structure, enhancing charge mobility (thin film transistor hole mobility is increased ~5 $\times$ ) and OPV performance (PCE is enhanced by ~2 $\times$ ). This study underscores the value of alkene functionalization and complements recent work by Miyanishi<sup>7</sup> on poly(3-hexenylthiophene) (P3HeT:PC<sub>61</sub>BM) OPVs. There higher mobility was observed vs P3HT:PC<sub>61</sub>BM, and microstructural stabilization could be further enhanced via C=C cross-linking.

Key to understanding the marked properties differences between **1** and **2** are the crystal structures. Crystals of each for diffraction were obtained by slow diffusion of orthogonal solvents (Figure 1). The molecular structures feature essentially planar cores extending from the central squaric rings to two of the four terminal phenyls and are characterized by *trans* *N*-substituted-pyrrolyl ring orientations (Figure 1B). The maximum torsions between the nearly coplanar pyrrolyl and phenyl rings are ~10° (**1**) and 25° (**2**), whereas the other two phenyl

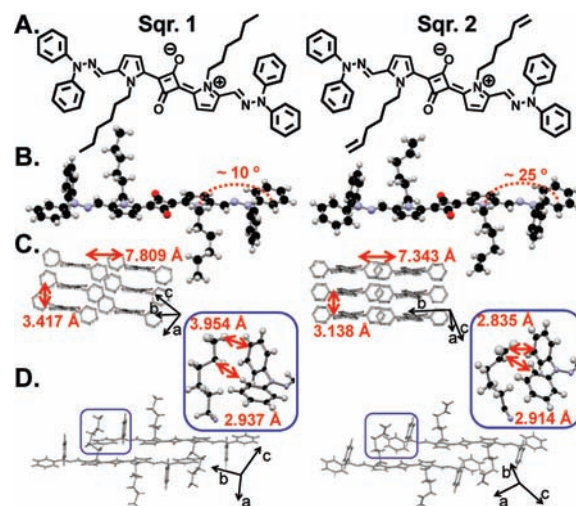


Figure 1. Molecular and crystal structures of squaraines **1** (right) and **2** (left).

rings project nearly perpendicular to the molecular planes in both molecules. Both squaraines crystallize in a cofacial motif (Figure 1), with minimum interplanar distances of 3.138 and 3.417 Å for **2** and **1**, respectively (Figure 1C); the former is smaller than the sum of C...C (3.30–3.40 Å) van der Waals radii.<sup>8</sup> The minimum interstack distance between cores is also significantly smaller for **2** (7.343 Å) than for **1** (7.809 Å), resulting in denser packing ( $d = 1.238$  for **2** vs  $1.215$  g/cm<sup>3</sup> for **1**). Importantly, this packing also features a very short edge- $\pi$  contact between the terminal hexenyl double bond and both phenyl rings in **2** (<3 Å, comparable to the sum of H...C (2.85–2.90 Å) van der Waals radii<sup>8</sup>) vs no contacts and larger distances between the saturated *n*-hexyl group and the analogous phenyl rings in **1** (3–4 Å, Figure 1D).

Figure S1 shows normalized optical spectra of **1**- and **2**-derived films cast from CHCl<sub>3</sub> solutions, of CHCl<sub>3</sub> solutions, and of BHJ blends with PC<sub>61</sub>BM and PC<sub>71</sub>BM. While the solution phase spectra are identical and exhibit typical sharp squaraine absorptions at 729 nm, the spectra of the pristine films are broad and span the 550–900 nm region with  $\lambda_{\text{max}}$  of **1** blue-shifted (660 nm) vs **2** (770 nm). Interestingly, the BHJ film optical spectra resemble those of the corresponding solutions but are slightly broadened, a signature of film microstructural details (vide infra). The HOMO and LUMO energies of **1** and **2**, estimated by cyclic voltammetry (Figure S2), are –3.3 and –5.0 eV, respectively, for both molecules, demonstrating that the alkyl/alkenyl chains negligibly affect solution redox properties. The HOMO and LUMO energies (Figure S3), absorption coefficients (~ $2 \times 10^5$  M<sup>-1</sup>cm<sup>-1</sup>), and absorption energies suggest that these new squaraines are promising electron donors for fullerene BHJ-OPVs.

<sup>‡</sup> Northwestern University.

<sup>¶</sup> Università di Perugia.

<sup>†</sup> Università di Milano-Bicocca.

<sup>§</sup> Polyera Corporation.

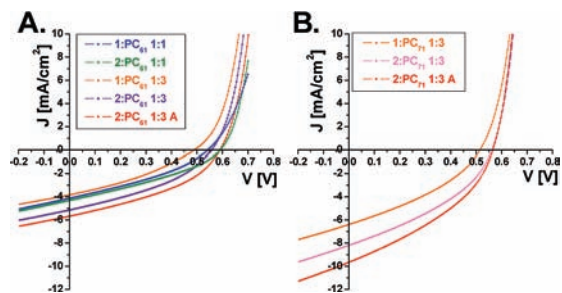


**Figure 2.** Average  $J$ - $V$  response of **1**- and **2**-based BHJ OPVs as a function of Sqr:PC<sub>xx</sub>BM ratio, with and without annealing, where PC<sub>xx</sub>BM is (A) PC<sub>61</sub>BM and (B) PC<sub>71</sub>BM.

**Table 1.** Comparison of Squaraine:PC<sub>xx</sub>BM BHJ Photovoltaic Cells<sup>a,b</sup>

Sqr./PC <sub>xx</sub> BM (wt:wt)	$d_{\text{ht}}^c$ [nm]	$D_{\text{al}}^d$ [nm]	$J_{\text{sc}}$ [mA/cm <sup>2</sup> ]	$V_{\text{oc}}$ [V]	FF [%]	PCE (PCE <sub>max</sub> ) [%]
1/PC <sub>61</sub> BM (1:1)	~50	~65	3.83	0.49	34	0.63 (0.68)
2/PC <sub>61</sub> BM (1:1)	~50	~65	4.31	0.59	34	0.87 (0.99)
1/PC <sub>61</sub> BM (1:3)	~75	~35	4.13	0.54	33	0.77 (0.78)
2/PC <sub>61</sub> BM (1:3)	~75	~35	5.15	0.56	37	1.10 (1.20)
1/PC <sub>61</sub> BM (1:3) <sup>e</sup>	~75	~35	5.68	0.59	39	1.34 (1.45)
1/PC <sub>71</sub> BM (1:3)	~75	~35	6.40	0.52	35	1.12 (1.29)
2/PC <sub>71</sub> BM (1:3)	~75	~35	8.21	0.56	37	1.72 (1.75)
1/PC <sub>71</sub> BM (1:3) <sup>e</sup>	~75	~50	7.16	0.55	37	1.39 (1.47)
2/PC <sub>71</sub> BM (1:3) <sup>e</sup>	~75	~35	9.32	0.57	37	1.99 (2.05)

<sup>a</sup> General device structure is ITO/PEDOT:PSS/Sq:PC<sub>xx</sub>BM blend/LiF/Al with ~6 mm<sup>2</sup> illuminated areas. <sup>b</sup> All devices characterized under the standard AM1.5G 1 Sun test conditions using instrumentation and analysis procedures described previously,<sup>4c</sup> and PCEs are derived from the equation  $\eta_p = (J_{\text{sc}}V_{\text{oc}}\text{FF})/P_0$ , where  $J_{\text{sc}}$  = the short circuit current [mA/cm<sup>2</sup>],  $V_{\text{oc}}$  the open circuit voltage [V], FF the fill factor, and  $P_0$  the incident light intensity [mW/cm<sup>2</sup>]. <sup>c</sup> Thickness of hole transport layer (PEDOT:PSS). <sup>d</sup> Thickness of active layer blend. <sup>e</sup> Annealed at 50 °C for 30 min.

BHJ-OPV cells were fabricated by spin-coating, under an ambient atmosphere, squaraine:acceptor (x:y wt:wt ratio) blends in CHCl<sub>3</sub> solution onto cleaned ITO-coated glass anodes, modified by first spin-coating on a PEDOT:PSS layer as a hole extraction/electron-blocking layer. After drying, the cells were then completed by sequential thermal vacuum deposition of LiF and Al as the cathode (Figure S4). Typical  $J$ - $V$  plots are shown in Figure 2, and EQE data for the best cell in Figure S5. Device optimization was accomplished by varying the PEDOT:PSS layer thickness, acceptor material (PC<sub>61</sub>BM or PC<sub>71</sub>BM), active layer thickness, and postdeposition thermal annealing (Tables S1–S3). Optimized OPV performance data are summarized in Table 1, with the PCE for **2** ~2% vs ~1.4% for **1**. From these data some general performance trends are clearly discerned: *i.* Replacing PC<sub>61</sub>BM with PC<sub>71</sub>BM significantly increases PCE (~2 ×). *ii.* Mild active layer thermal annealing (50 °C) before device completion enhances performance by increasing  $J_{\text{sc}}$ . *iii.* Hexenyl-substituted squaraine **2**-based devices invariably outperform those based on hexyl-substituted **1**. Since the  $V_{\text{oc}}$  (~0.55 V) and FF (~35%) of all devices are similar, the performance differences predominantly arise from  $J_{\text{sc}}$  enhancement.

Regarding the origin of the OPV response trends, AFM data for the BHJ blends (Figures S6,S7) argue that the enhanced PC<sub>71</sub>BM-based device performance results from not only the greater light harvesting capacity of this acceptor but also greater microstructural ordering vs the PC<sub>61</sub>BM-based films. The 1-/2-PC<sub>61</sub>BM films exhibit negligible donor–acceptor phase separation, with the film morphology resembling solid solutions (Figures S6B,S7B), whereas the 1-/2-PC<sub>71</sub>BM films are characterized by 20–30 nm wide squaraine fibrils embedded in the fullerene matrix (Figures S6C,S7C). Interestingly, the 1- and 2-PC<sub>71</sub>BM blend AFM images are practically identical, meaning the enhanced PCE of the former system is not exclusively morphological in origin. Rather, the enhanced hole transport of the **2**

vs **1** squaraine nanofibrils may be due to the denser, more compact **2** microstructure, which provides the principal overall current enhancement. To test this hypothesis, thin-film transistors based on **1** and **2** were also fabricated. These exhibit average field-effect hole mobilities of  $(2.7 \pm 1.8) \times 10^{-5}$  and  $(1.2 \pm 0.2) \times 10^{-4}$  cm<sup>2</sup>/(V s), respectively, indicating **2** is a more efficient hole transporter than **1** (Figure S8), as suggested by the structural analysis.

In summary, we report the fabrication and initial characterization of BHJ solar cells based on alkyl- and alkenyl-functionalized squaraine dyes as donors, with PC<sub>61</sub>BM and PC<sub>71</sub>BM as acceptors. These devices, solution-processed in ambient, exhibit the highest PCEs within the squaraine donor family and surpass those of several other molecular donor families. More importantly, we demonstrate and rationalize a new structural strategy, via noncovalent alkenyl-phenyl contacts, to enhance charge transport efficiency in squaraine-based OPVs. We believe that this approach can be extended to other molecular and polymeric semiconductors as well.

**Acknowledgment.** We thank DOE (DE-FB02-08ER46536-/A000) for support of this research, the Northwestern U. MRSEC (NSF DMR-0520513) for providing characterization facilities, and Ms. M. Ferrari for sample preparation and helpful discussions.

**Supporting Information Available:** Synthetic procedures for **1** and **2**; device fabrication and characterization details; optical spectra of **1**, **2**, and blends; and AFM images of films. This material is available free of charge via the Internet at <http://pubs.acs.org>.

## References

- (a) Po, R.; Maggini, M.; Camaioni, N. *J. Phys. Chem. C* **2010**, *114* (2), 695. (b) Bredas, J.-L.; Norton, J. E.; Cornil, J.; Coropceanu, V. *Acc. Chem. Res.* **2009**, *42* (11), 1691. (c) Gommans, H.; Aernouts, T.; Verreert, B.; Heremans, P.; Medina, A.; Claessens, C. G.; Torres, T. *Adv. Funct. Mater.* **2009**, *19* (21), 3435. (d) Brabec, C. J.; Durrant, J. R. *MRS Bull.* **2008**, *33*, 670. (e) Kroon, R.; Lenes, M.; Hummelen, J. C.; Blom, P. W. M.; de Boer, B. *Polym. Rev.* **2008**, *48*, 531. (f) Kim, J. Y.; Lee, K.; Coates, N. E.; Moses, D.; Nguyen, T. Q.; Dante, M.; Heeger, A. J. *Science* **2007**, *317*, 222. (g) Hoth, C. N.; Choulis, S. A.; Schilinsky, P.; Brabec, C. J. *Adv. Mater.* **2007**, *19*, 3973. (h) Li, G.; Shrotriya, V.; Huang, J.; Yao, Y.; Moriarty, T.; Emery, K.; Yang, Y. *Nat. Mater.* **2005**, *4*, 864. (i) Rand, B. P.; Genoe, J.; Heremans, P.; Poortmans, J. *Prog. Photovoltaics* **2007**, *15*, 659. (j) Lloyd, M. T.; Anthony, J. E.; Malliaras, G. G. *Mater. Today* **2007**, *10*, 34.
- (a) Armstrong, N. R.; Veneman, P. A.; Ratcliff, E.; Placencia, D.; Brumbach, M. *Acc. Chem. Res.* **2009**, *42*, 1748. (b) Potscavage, W. J., Jr.; Sharma, A.; Kippelen, B. *Acc. Chem. Res.* **2009**, *42*, 1758. Thompson, B. C.; Frechet, J. M. J. *Angew. Chem., Int. Ed.* **2008**, *47*, 58. Yip, H.-L.; Hau, S. K.; Baek, N. S.; Ma, H.; Jen, A. K.-Y. *Adv. Mater.* **2008**, *20*, 2376. (c) Riede, M.; Mueller, T.; Tress, W.; Schueppel, R.; Leo, K. *Nanotechnology* **2008**, *19*, 424001. (d) Padinger, F.; Rittberger, R. S.; Sariciftci, N. S. *Adv. Funct. Mater.* **2003**, *13*, 85. (e) Shaheen, S. E.; Brabec, C. J.; Sariciftci, N. S. *Appl. Phys. Lett.* **2001**, *78*, 841.
- Wang, S.; Mayo, E. I.; Perez, M. D.; Griffe, L.; Wei, G.; Djurovich, P. I.; Forrest, S. R.; Thompson, M. E. *Appl. Phys. Lett.* **2009**, *94*, 233304.
- (a) Park, S. H.; Roy, A.; Beaupré, S.; Cho, S.; Coates, N.; Moon, J. S.; Moses, D.; Leclerc, M.; Lee, K.; Heeger, A. J. *Nat. Photonics* **2009**, *3*, 297. (b) Puetzner, S.; Meiss, J.; Petrich, A.; Riede, M.; Leo, K. *Appl. Phys. Lett.* **2009**, *94*, 223307. (c) Irwin, M. D.; Buchholz, B.; Hains, A. W.; Chang, R. P. H.; Marks, T. J. *Proc. Natl. Acad. Sci. U.S.A.* **2008**, *105*, 2783. (d) Valentini, L.; Bagnis, D.; Kenny, J. M. *Nanotechnology* **2009**, *20*, 095603. (e) Hains, A. W.; Marks, T. J. *Appl. Phys. Lett.* **2008**, *92*, 023504/1–023504/3.
- (a) Liang, Y.; Feng, D.; Wu, Y.; Tsai, S.-T.; Li, G.; Ray, C.; Yu, L. *J. Am. Chem. Soc.* **2009**, *131*, 7792. (b) Zou, Y.; Gendron, D.; Neagu-Plesu, R.; Leclerc, M. *Macromolecules* **2009**, *42*, 6361. (c) Chen, M.-H.; Hou, J.; Hong, Z.; Yang, G.; Sista, S.; Chen, L.-M.; Yang, Y. *Adv. Mater.* **2009**, *21*, 4238. (d) Walker, B.; Tamayo, A. B.; Dang, X.-D.; Zalar, P.; Seo, J. H.; Garcia, A.; Tantiwiwat, M.; Nguyen, T. Q. *Adv. Funct. Mater.* **2009**, *19*, 1. (e) Sreejith, S.; Carol, P.; Chithra, P.; Ajayaghosh, A. *J. Mater. Chem.* **2008**, *18*, 264. (f) Valentini, L.; Bagnis, D.; Marrocchi, A.; Seri, M.; Taticchi, A.; Kenny, J. M. *Chem. Mater.* **2008**, *20*, 32.
- (a) Silvestri, F.; Irwin, M. D.; Beverina, L.; Facchetti, A.; Pagani, G. A.; Marks, T. J. *J. Am. Chem. Soc.* **2008**, *130*, 17640. (b) Beverina, L.; Crippa, M.; Landenna, M.; Ruffo, R.; Salice, P.; Silvestri, F.; Versari, S.; Villa, A.; Cifroni, L.; Collini, E.; Ferrante, C.; Bradamante, S.; Mari, C. M.; Bozio, R.; Pagani, G. A. *J. Am. Chem. Soc.* **2008**, *130*, 1894. (c) Beverina, L.; Abbotto, A.; Landenna, M.; Cerminara, M.; Tubino, R.; Meinardi, F.; Bradamante, S.; Pagani, G. A. *Org. Lett.* **2005**, *7*, 4257.
- Miyaniishi, S.; Tajima, K.; Hashimoto, K. *Macromolecules* **2009**, *42*, 1610.
- Huhey, J. E.; Keiter, A. Keiter, R. L. *Inorganic Chemistry*; Harper Collins College Publishers: New York, 1993.

JA100520Q